https://doi.org/10.5194/wcd-2021-9
Preprint. Discussion started: 10 February 2021

Weather and Climate Dynamics Discussions
Open Access
EGU

Mechanisms driving MJO teleconnection changes with warming in CMIP6

Andrea M. Jenney[1], David A. Randall[2], and Elizabeth A. Barnes[2]

[1]Department of Earth System Science, University of California, Irvine, CA, USA
[2]Department of Atmospheric Science, Colorado State University, Fort Collins, CO, USA

Correspondence: Andrea M. Jenney (ajenney@uci.edu)

Abstract. Teleconnections from the Madden-Julian Oscillation (MJO) are a key source of predictability of weather on the extended time scale of about 10-40 days. The MJO teleconnection is sensitive to a number of factors, including the mean state dry static stability, the mean flow, and the propagation and intensity characteristics of the MJO itself, which are traditionally difficult to separate across models. Each of these factors may evolve in response to increasing greenhouse gas emissions, which will impact MJO teleconnections and potentially impact potential predictability on extended time scales. Current state-of-the-art climate models do not agree on how MJO teleconnections will change in a future climate. Here, we use results from the Coupled Model Intercomparison Project Phase 6 (CMIP6) historical and SSP585 experiments in concert with a linear baroclinic model to separate and investigate alternate mechanisms explaining why and how MJO teleconnections over the North Pacific and North America will change in a future climate, and to identify key sources of inter-model uncertainty. We find that decreases to the MJO teleconnection due to increases in tropical dry static stability alone are robust, and that uncertainty in mean state winds are a key driver of uncertainty in future MJO teleconnections. We find no systematic relationship between changes in Rossby wave excitation and the MJO teleconnection. However, we find that models that predict increases (decreases) in the stationary Rossby wave number over the gulf of Alaska also predict stronger (weaker) teleconnections over North America. Uncertainty in future changes to the MJO's intensity, eastward propagation speed, and eastward propagation extent are other important sources of uncertainty in future MJO teleconnections, although to a lesser degree than uncertainty in the mean state. The overall outlook is a reduction of the boreal winter MJO teleconnection across the vast majority of CMIP6 models, especially over the North Pacific, but with some nuance over North America due to larger sensitivity to expansion of the MJO's eastward extent.

1 Introduction

As the most energetic mode of tropical intraseasonal variability, the Madden-Julian Oscillation (MJO) is one of the most important sources of global weather predictability on the extended time range of about 10-40 days (Robertson et al., 2015). Its

https://doi.org/10.5194/wcd-2021-9
Preprint. Discussion started: 10 February 2021

impact on remote weather is sensitive to a number of factors including the static stability of the tropics, the magnitude of the MJO's convective and radiative heating anomalies, its propagation speed, the eastward extent of MJO convective propagation, and the mean state winds, each of which may evolve in response to increased atmospheric greenhouse gas concentrations. There is a considerable amount of uncertainty in the response of many of these features to warming. Additionally, cloud parameterizations and coarse grid spacing lead to a relatively poor simulation of the MJO in many climate simulations (Ahn et al., 2017). It is thus unclear how the influence of the MJO over much of the extratropics will change in a future warmer climate (Zhou et al., 2020).

Whereas some consensus has been emerging about at least one of these controls that affects MJO teleconnection strength–the increase of the tropical dry static stability with surface warming –recent studies suggest this control may be secondary. To first order, the rate that air rises and sinks in the MJO's circulation is tightly constrained by, and inversely proportional to, the tropical dry static stability (Wolding et al., 2016). Latent heat release associated with MJO precipitation is balanced by the upward advection of dry static energy. Similarly, radiative cooling in the MJO's dry region is balanced by slow, adiabatic subsidence. It is expected that the tropical static stability will increase in the future as the tropical temperature profile adjusts towards the moist adiabatic lapse rate of a warmer surface. Ignoring changes to the MJO's precipitation intensity or its cloud optical properties, this will weaken the MJO's vertical circulation and its associated upper-level divergence. In simulation studies of a future climate forced with increasing greenhouse gases, many models predict a weakening of the MJO's circulation strength (Bui and Maloney, 2018; Maloney et al., 2019). However, there is a considerable amount of inter-model spread, much of which is tied to disagreement in future projections of the MJO's diabatic heating and precipitation (Bui and Maloney, 2018; Maloney et al., 2019; Bui and Maloney, 2019a, b). While previous work has attributed a simulated weakening of MJO teleconnections in one model to the increase in dry static stability (Wolding et al., 2017), a recent model intercomparison study has shown that in climate change simulations the MJO's circulation change is not correlated with its teleconnection changes (Zhou et al., 2020).

We hypothesize that the lack of an apparent relationship between modeled MJO circulation change and teleconnection change may be related to changes in the mean state winds. Mean state winds refer to the winds that vary slowly in time (i.e., on seasonal, rather than daily time scales). Henderson et al. (2017) emphasize the importance of the mean state winds in the MJO teleconnection pattern, showing that biases in modeled MJO teleconnections can be attributed, in part, to biases in the mean state winds. Mean state winds affect both Rossby wave excitation and their propagation. The magnitude of the vorticity and its horizontal gradient on the equatorward flank of the jet play an important role in the excitation of Rossby waves by the MJO (Sardeshmukh and Hoskins, 1988; Mori and Watanabe, 2008; Seo and Son, 2012; Seo and Lee, 2017). The jets also act as a waveguide, and their structure and intensity determine the path that Rossby waves take as they propagate, and the sizes of Rossby waves that can propagate through them (e.g., Hoskins and Ambrizzi, 1993; Karoly, 1983). Tseng et al. (2020b) show that differences in Rossby wave propagation, due to differences in mean state winds over the eastern Pacific, drives most of the interannual variability in the MJO teleconnection pattern over the northern Pacific and North America region. Zhou et al. (2020) show that modeled increases in the MJO's impact over the North American west coast with warming are due to an extension of the Pacific jet, which causes a shift in the MJO teleconnection pattern. However, little work has been done to

https://doi.org/10.5194/wcd-2021-9
Preprint. Discussion started: 10 February 2021

explore the direct role that changes to the mean state winds have on changing MJO teleconnections to the broader North Pacific and North America region.

In addition to features of the mean state (its static stability and winds), the MJO teleconnection may also respond to changes in the MJO itself. The MJO teleconnection is known to be sensitive to its eastward propagation speed. In a simulation study, Bladé and Hartmann (1995) showed that an eastward propagating heat source is associated with a weaker and smaller wavetrain than a stationary or westward propagating heat source. To first order, this is a linear effect: eastward (westward) propagation effectively embeds the heating in easterlies (westerlies) (see Sect. 2b of Bladé and Hartmann, 1995). Many climate models predict an increase in the MJO's propagation speed with warming (e.g., Rushley et al., 2019), which may contribute to a weakening of the MJO teleconnection with warming.

In the present climate, MJO convection is generally confined to the Indian and West Pacific oceans, while the MJO circulation signal circumnavigates the tropics. In simulations of a future warmer climate, many models predict an increase in the eastward extent of MJO convection (Adames et al., 2017; Bui and Maloney, 2018; Chang et al., 2015; Subramanian et al., 2014). This may be driven by the expansion of the eastward edge of the Indo-Pacific warm pool, a region of very warm tropical sea surface temperatures (Maloney and Xie, 2013; Zhou et al., 2020). A more eastward propagating MJO will extend the region of Rossby wave excitation by the MJO further eastward as well.

Studies exploring the teleconnection change with warming in global climate models are sparse. While Zhou et al. (2020) show that a multi-model mean MJO teleconnection change over North America is near-zero, they do not quantify the uncertainty in this projection over this larger region. Their results for the North American west coast, which rely on a subset of the publicly available climate model data (they analyze only those models that produce the most realistic MJOs), hint that while the multi-model mean change over broader North America is small, there may be quite a bit of disagreement between models.

The importance of the MJO's teleconnection for making predictions on extended timescales, combined with the MJO teleconnection's complex dependence on a number of climate features makes a detailed study of potential MJO teleconnection changes attractive. We are motivated to unpack how and why MJO teleconnections might change under global warming, and here seek to clearly and quantitatively rank the various controls on MJO teleconnection changes in a warmer climate to better understand how the MJO teleconnection might change in the future. Additionally, we desire to maximize the resources offered by the latest phase of the Coupled Model Intercomparison Project (CMIP6), by avoiding having to subset only those models producing more realistic MJOs.

In this study, we will use a linear baroclinic model (LBM, Watanabe and Kimoto, 2000) in concert with output from CMIP6 to test the hypothesis that the uncertainty in projections of the boreal winter MJO teleconnection to the North Pacific and North America region is large, and to separately quantify the contribution to this uncertainty by various mechanisms. The use of the LBM for studying the MJO teleconnection has precedent: Previous work has shown that the MJO teleconnection is, to first order, and the LBM is a common tool used to untangle MJO teleconnection mechanisms (e.g., Henderson et al., 2017; Tseng et al., 2019, 2020a, b; Wang et al., 2020; Wolding et al., 2017). The linear model additionally has a few features that make it particularly attractive for the current study. First, it is very inexpensive to run, allowing us to cheaply and efficiently run hundreds of perturbation simulations, a task that is difficult and expensive using complex global climate models. Second, the

https://doi.org/10.5194/wcd-2021-9
Preprint. Discussion started: 10 February 2021

Weather and Climate Dynamics Discussions
Open Access
EGU

linear framework is quite simple in that almost all simulated variability is due to the addition of an external forcing, which makes the interpretation of the results very straightforward. Third, because the mean state is maintained by prescribing it at each time step, it is possible to run simulations with the temperature field out of balance with the wind field. This final point allows us to separately and cleanly quantify the uncertainty in the MJO teleconnection change from uncertainty in the thermal structure of the atmosphere versus its mean winds.

2 Methods

We explore the sensitivity of the MJO teleconnection to changes in the MJO's propagation speed, eastward propagation extent, heating magnitude, and of the mean state dry static stability and winds using simulations with the LBM of Watanabe and Kimoto (2000). The time-integration version of the LBM that we use here is a spectral model that solves linearized equations for vorticity, divergence, temperature, and surface pressure. The model takes two inputs: a mean state and a forcing (which is added to the simulated perturbation field at each time step).

The model equations are described in appendix B of Watanabe and Kimoto (2000). The model is numerically damped with biharmonic horizontal diffusion, for which we use an e-folding time of 10 minutes for the smallest resolvable waves, and with linear drag, with a damping time scale of 0.5 days applied to the lowest 3 model levels, 1 day for the top two model levels, and 20 days for all levels in between. We use this strong damping to inhibit the growth of baroclinic waves, particularly because in some simulations we intentionally prescribe mean state winds that are not in balance with the mean state temperature. We use a horizontal truncation of T42 (roughly 2.8° horizontal resolution) and 20 vertical levels.

We will make the convention for composite analysis that "historical" and "future" mean states refer to January conditions during 1984-2014, and 2071-2100, respectively, of the historical and SSP585 simulations from models participating in CMIP6. SSP585 is a relatively high atmospheric greenhouse gas emissions scenario following shared socioeconomic pathway 5 (SSP5; O'Neill et al., 2017) and representative concentration pathway 8.5 (Moss et al., 2010). For each CMIP6 model mean state combination, we construct an ensemble of 30 separate LBM simulations, each using a different January. We use interannual ensembles in this way to isolate the climate change signal apart from noise due to internal variability.

We restrict our analysis to those 29 CMIP6 models for which there was monthly mean data for the variables required as input by the LBM on the data node at https://esgf-node.llnl.gov/search/cmip6/ at the time of access. We use the r1i1p1f1 variant for all models except for GISS-E2-1-G (r1i1p1f2), HADGEM3-GC31-LL (r1i1p1f3), UKESM1-0-LL (r1i1p1f2), and MIROC-ES2L (r1i1p1f2). Lastly, the SSP585 simulation of CAMS-CSM1-0 was only carried out until 2099, and so for this model we use only 29 ensemble members.

We force the LBM with a propagating idealized horizontal dipole heating, which is preferable to a realistic heat source (for example, one obtained from composites of observed MJO events), since it allows easily manipulation of the MJO's intensity

https://doi.org/10.5194/wcd-2021-9
Preprint. Discussion started: 10 February 2021

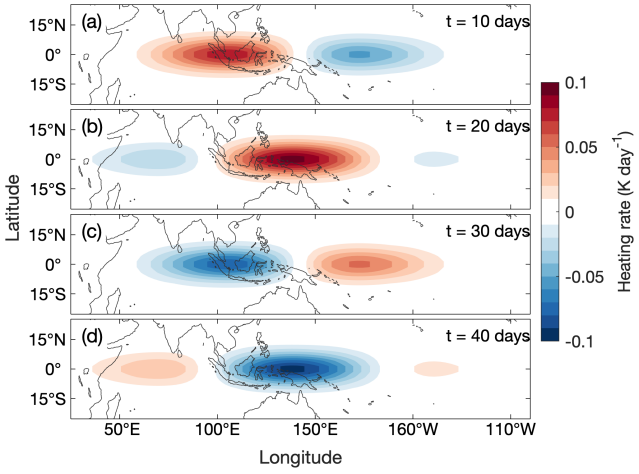

Figure 1. Propagating thermal forcing used in the LBM simulations at t = (a) 10 days, (b) 20 days, (c) 30 days, and (d) 40 days.

and propagation characteristics. The heating is designed to be MJO-like, with the rate of change of perturbation temperature given by

$$\frac{\partial T'(\lambda,\phi,z,t)}{\partial t} = Ae^{\frac{-\sin^2\phi}{2\sigma^2}}\sin(k\lambda-\omega t)e^{\frac{-(\lambda-b)^2}{2c^2}}\sin^2\left(\frac{\pi(z-z_{top})}{z_{bot}-z_{top}}\right), \quad (1)$$

where T' is the perturbation temperature of the forcing, ϕ and λ are the latitude and longitude, respectively, z is the model vertical coordinate with subscripts bot and top referring to the lowest and highest model level, respectively, A is the heating amplitude, k is the zonal wavenumber, ω is the temporal frequency of the heating, and t is the time. Unless otherwise noted, we set A = 0.1 K day^{-1}, σ = 0.1, k = 1.9, ω corresponding to a temporal period of 40 days, b = 130°, and c = 45°. Figure 1 shows the heating in the mid-troposphere where it is a maximum for t = 10 days, 20 days, 30 days, and 40 days. To impose a realistic MJO horizontal scale, and facilitate varying it, we constrain the propagating heat source to the longitudes over the Indian and West Pacific Oceans by multiplying the sinusoidal heat source by a Gaussian centered over the Maritime continent (see Eq. 1). We initialize the model with the forcing given by setting t = 1 day, and integrate for 60 days.

The experiments are described in Table 1. When testing the sensitivity of the MJO teleconnection to perturbations of the mean state or of an MJO intensity or propagation characteristic, we perturb only the feature being tested and hold everything else constant. For each perturbed feature, we run two sets of experiments: one with a mean state given by historical values, and the other with the mean state given by future values (see the "sub-experiment" column in Table 1). For example, in testing the sensitivity of the teleconnection to the mean state winds, we run two sets of experiments: one in which the dry static stability is held constant at historical values and the other with future dry static stability. The use of the many CMIP6 mean states permits the quantification of uncertainty in the future MJO teleconnection due to "model uncertainty" (e.g., Lehner et al., 2020) of the mean state.

https://doi.org/10.5194/wcd-2021-9
Preprint. Discussion started: 10 February 2021

Table 1. Experimental setup for the linear baroclinic model simulations. "Lower bound" and "upper bound" refer only to perturbations of the thermal forcing (last three rows). DSE = dry static energy.

Feature	Sub-experiment	Control	Perturbation (lower bound)	(upper bound)	Number of unique simulations	Number of unstable simulations
Mean state DSE	Historical wind	Historical DSE	Future DSE		1440	49
	Future wind				1440	63
Mean state winds	Historical DSE	Historical wind	Future wind			
	Future DSE					
Forcing heating magnitude	Historical mean state	A = 0.10 K day^{-1}	A = 0.09 K day^{-1}	A = 0.12 K day^{-1}	60	0
	Future mean state				60	0
Forcing propagation speed	Historical mean state	ω = 1/40 day^{-1}	ω = 1/37.5 day^{-1}	ω = 1/34 day^{-1}	600	0
	Future mean state				600	0
Forcing eastward extent	Historical mean state		0° extension	20° extension	600	0
	Future mean state				600	1

We are guided by the results of previous studies for the experiments where the full mean state is held constant and MJO intensity or propagation characteristics are being perturbed. For these simulations, we aim to quantify uncertainty by obtaining the range of possible changes to the MJO teleconnection that result from changes to the MJO. We do this by conducting experiments with perturbations representing the lower and upper bound of changes to the MJO that are expected in a future warmer climate. For climate models that simulate realistic MJOs in the Coupled Model Intercomparison Project Phase 5 (CMIP5), Rushley et al. (2019) find an increase in MJO propagation speed between 1.8 and 4.5 % K^{-1}. Using the increase of the multi-model mean, global mean surface temperature between the historical and future climates of the models used in this study, we thus conduct experiments where the propagation speed of our idealized forcing is perturbed to correspond to an MJO period of about 37.5 (34) days for the lower bound (upper bound) experiment where sensitivity to MJO propagation speed is being tested. In modification of the MJO's eastward extent, we use no change as a lower bound and for the upper bound, extend by 20° the eastern edge of the gaussian used to confine the propagating forcing to the Indian and West Pacific Oceans. Specifically, the gaussian multiplier of the perturbation forcing is the control gaussian with the maximum value sustained for an additional 20° to the east before decreasing. Lastly, we are informed by Bui and Maloney (2018), who find that the subset of CMIP5 models that produce MJOs validating best against present-day observations tend to simulate changes of the MJO's precipitation amplitude between -10% to + 20% between the historical and future climates under RCP8.5 forcing. In the experiment testing sensitivity to MJO amplitude, we use perturbed MJO heating amplitudes of 0.9 and 0.12 K day^{-1}, corresponding to a 10% reduction and 20% amplification of the control forcing.

https://doi.org/10.5194/wcd-2021-9
Preprint. Discussion started: 10 February 2021

With the described setup, some of the simulations became unstable. We readily admit this is an inescapable trade-off of having assumed a forced linear model framework; despite its advantages for rapidly sampling and intercomparing first-order effects, the neglect of secondary nonlinear buffering mechanisms can corrupt some integrations. Pragmatically, we thus omit all LBM simulations in which, at any location, the maximum value during the second half of the integration is more than ten times the maximum value during the first half. Additionally, we omit all LBM simulations using a specific CMIP6 model's mean state if 10 or more of the 30 constituent ensemble simulations for any of the mean state combinations meets the instability criterion described above, leaving 24 of the 29 CMIP6 models for analysis. Figure A1 in Appendix A shows, for each basic state combination, the fraction of ensemble members that became unstable. The last two rows of Table 1 list the number of total simulations run for this study (minus those from the five CMIP6 models we omit) and the number of simulations we omit from our analysis for each experiment (which is reassuringly less than 5% of the total simulations for each experiment). Note that the "number of unique simulations" field is blank for the mean state winds feature (second row) because the simulations are shared with that of mean state dry static stability (first row).

3 Results

3.1 Mean state

We conduct experiments with the experimental setup described by Table 1.

Reassuringly, the propagating MJO-like forcing in the model excites a plausible time-varying response in the extratropics. For the set of 30 simulations performed with the full mean state given by historical values from a single representative CMIP6 model (ACCESS-ESM1-5), Fig. 2a shows the time-varying response of 850 hPa meridional wind at 52° N, 120° W for each ensemble member (thin light blue lines) and their mean (thick black line). The smallness of the meridional wind anomalies relative to a typical observed midlatitude value is an expected consequence of the smallness of the amplitude used to force the model, which we kept small to try to minimize the number of unstable simulations.

We next introduce a scalar metric of MJO teleconnection strength that is appropriate to visualize in map form, recognizing that the magnitude of peaks and troughs of the ensemble mean response to the propagating forcing in Fig. 2a is one way to quantify the magnitude of the consistent (ensemble mean signal that stands apart from the noise due to internal variability) teleconnection strength. Given that the amplitude of an infinite sine or cosine wave is the square root of twice its variance, we calculate the teleconnection strength at each point as the square root of twice the variance of the ensemble mean meridional wind at 850 hPa, ignoring the first 10 days of each simulation to avoid sampling conditions prior to the establishment of representative spread between interannually varying ensemble members. We will refer to this value as the "amplitude" of the modeled MJO teleconnection. This metric is qualitatively similar to the STRIPES index of Jenney et al. (2019), but is more simple because the forcing is identical between each simulation in an ensemble set, and because the propagating forcing is the sole source of variability in the LBM simulations. We use low-level meridional wind in this calculation (instead of other dynamically relevant variables like mid-tropospheric geopotential height, for example), because the MJO primarily drives

https://doi.org/10.5194/wcd-2021-9
Preprint. Discussion started: 10 February 2021

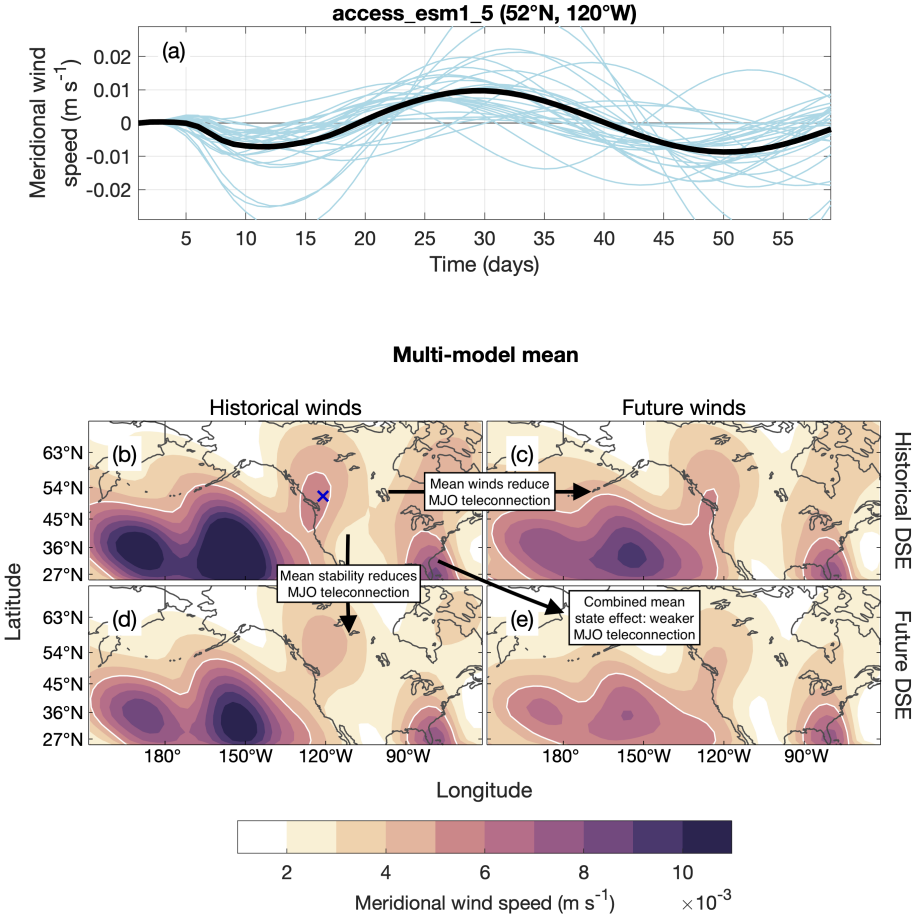

Figure 2. (a) The time series of meridional wind at 850 hPa at 52° N, 120° W for each January and their mean (thick black line) for the set of LBM simulations with the historical mean state winds and dry static energy (DSE) from ACCESS-ESM1-5. (b) The multi-model mean of the square root of twice the variance of each model's ensemble mean meridional wind at 850 hPa for the set of simulations with mean states given by historical winds and DSE, (c) future winds and historical DSE, (d) historical winds and future DSE, and (e) future winds and DSE. The blue "x" in panel (b) is the location shown in panel (a). The white lines in panels (b)-(d) indicate the 5 $\times 10^{-3}$ contour. DSE = dry static energy.

surface temperature variability across North America via low-level temperature advection (Seo et al., 2016), and may thus be more relevant for quantifying changes to the MJO's *impact* on near-surface midlatitude weather in a future climate.

The baseline multi-model MJO teleconnection looks reassuringly plausible. Figure 2b shows the multi-model mean MJO teleconnection amplitude for the set of simulations performed with both the mean state dry static energy (the vertical gradient of which gives the dry static stability) and winds given by historical values. Darker colors indicate that MJO teleconnectivity is larger. The MJO-like forcing excites Rossby waves that propagate in high density through the Pacific waveguide, leading to large values of teleconnectivity there. The pattern of MJO teleconnectivity over North America, which exhibits maxima over

https://doi.org/10.5194/wcd-2021-9
Preprint. Discussion started: 10 February 2021

the southeastern and northwestern region, with a minimum over the central region, is consistent with the pattern of the observed boreal winter MJO influence on North American temperature (e.g., Jenney et al., 2019; Zhou et al., 2012).

The remainder of Fig. 2 reveals an overall reduction of MJO teleconnectivity due to future mean state effects, decomposed into separate contributions from stability vs. winds. Figure 2c-e shows the amplitude of the modeled MJO teleconnection but for the set of simulations performed by perturbing the mean state. The forcing used in all simulations is the same. The difference between the top and bottom rows is the sensitivity of the MJO teleconnection to the change in the thermal structure of the atmosphere (i.e., its dry static stability), alone. The pattern of the MJO teleconnection is the same between each top panel and the panel below it, but the teleconnection is weaker in the simulations with future dry static energy because the higher static stability weakens the MJO circulation and subsequent Rossby wave source (Sardeshmukh and Hoskins, 1988) that results from the prescribed thermal forcing. The difference between the left column and the right column is the sensitivity of the MJO teleconnection amplitude to the simulated change in mean winds between the historical and future climates of CMIP6. For most regions, the change to the mean state winds between the historical and future climates leads to a reduction of the MJO teleconnection amplitude. This reduction is particularly apparent over the central Pacific. Other studies have noted an increase in the MJO's boreal winter influence near California (Zhou et al., 2020), attributing this to an eastward extension of the Pacific jet. Here, we find a similar strengthening over this region. In Fig. 2c-e, we include a white line highlighting the 5 $\times 10^{-3}$ m s^{-1} contour to help show this strengthening, which is apparent as an eastward extension of this contour line towards the California coast.

The difference between panels (b) and (e) of Fig. 2 is the sensitivity of the MJO teleconnection to a change in the full mean state, neglecting any changes to the MJO. In isolation (apart from changes to the MJO), changes to the mean state weaken the multi-model mean teleconnection amplitude almost everywhere due to both an intensification of the dry static stability and changes to the winds.

We now explore the inter-model spread of changes to the MJO teleconnection due to changes in the mean state. Figure 3a,c summarizes, for the separate mean states from each CMIP6 model, the change in the LBM-simulated teleconnection amplitude over the North Pacific (top panels; 150°-235° E, 25°-70° N) and North America (bottom panels; 25°-70° N and 235°-290° E, 25°-70° N), as a percent change per Kelvin multi-model mean warming. For each region we plot the domain-mean percent change in the teleconnection amplitude, as well as the fractional area that is strengthening. We include the fractional area as a crude way to communicate the spatial distribution of teleconnection changes over the region. For example, in isolation, the mean teleconnection amplitude change over the region may be misleading if one small region experiences a very strong change in one direction (enough to make the domain mean change be of the same sign), despite the majority of the domain experiencing a change of the opposite direction. For example, there are a few models in panel b which lie to the right of the vertical zero line (indicating a mean *positive* change in the teleconnection amplitude over the North Pacific due to the winds alone) and to the bottom of the horizontal zero line (indicating that a majority fraction of the region shows a *weakening*).

Our first main finding is strong corroboration of the hypothesis that the increase of the tropical dry static stability is a robust thermodynamic response of the climate to warming that tends to reduce the MJO's teleconnections in almost all models. This is the first multi-model confirmation of this hypothesis, which first appears in the single-model study of Wolding et al. (2017).

https://doi.org/10.5194/wcd-2021-9
Preprint. Discussion started: 10 February 2021

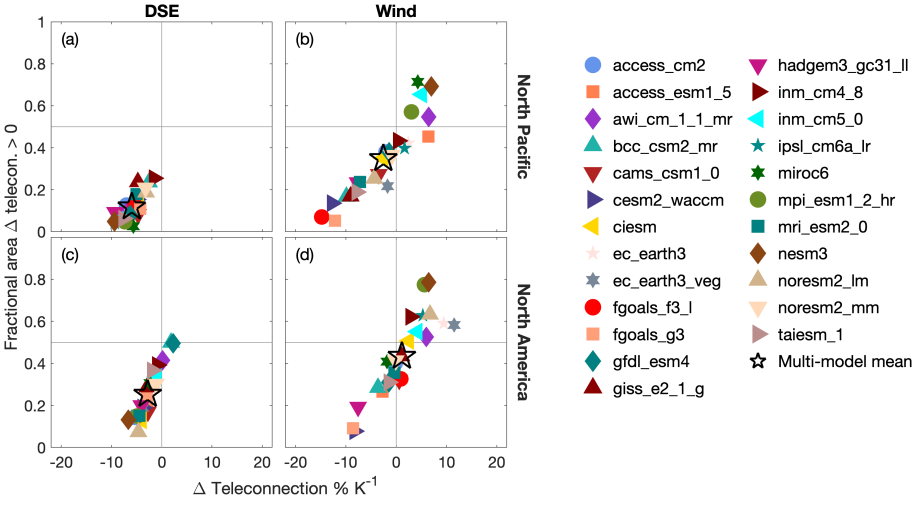

Figure 3. For individual CMIP6 model mean states and the multi-model mean, the change in the teleconnection amplitude (as a percent change per multi-model mean Kelvin warming) to the North Pacific (150°-235° E, 25°-70° N) and North America (235°-290° E, 25°-70° N) between LBM simulations with mean states given by future and historical quantities. The isolated change due to (a) stability, over the North Pacific; (b) wind, over the North Pacific; (c) stability, over North America; (d) wind, over North America. Horizontal axis is the domain mean change over the region, while the vertical axis shows the fractional area of teleconnection amplitude strengthening. DSE = dry static energy.

There is relatively good agreement in the teleconnection amplitude change between model mean states, particularly over the North Pacific. Comparison between panels a and c of Fig. 3 shows that there is greater spread downstream of the tropical heat source over North America, although reasons for this are unclear.

Despite agreeing on effects of stability, models disagree wildly on the effects of future wind changes. Figure 3b,d show the change in the teleconnection amplitude due to the change in the wind between the historical and future period. The multi-model mean response of the MJO teleconnection amplitude over the North Pacific is a modest weakening, with a majority of the region also experiencing a weakening. However, the inter-model spread is relatively large, with models showing changes between -15 to 7 % K^{-1} multi-model mean warming. Over North America, the multi-model mean change in the teleconnection due to the wind is a small strengthening, with most of the region showing weaker teleconnections. But again, the inter-model spread is large (-9 to 12 % K^{-1}) with the multi-model mean is indistinguishable from zero as was found in Zhou et al. (2020).

In summary, three key results emerge concerning how mean state changes in a future warmer climate will contribute to changing MJO teleconnections to the North Pacific and North America. First, we find robust support for the expectation that increases in tropical dry static stability will contribute to weaker MJO teleconnections. Second, we find that changes to the mean state winds can contribute to very large changes in the MJO teleconnection; that is, large enough to as much as double or negate the weakening that is expected due to increasing tropical dry static stability. Third, there is a large amount of inter-model spread in LBM-simulated changes to the MJO teleconnection that result from changes to mean state winds, which suggests

https://doi.org/10.5194/wcd-2021-9
Preprint. Discussion started: 10 February 2021

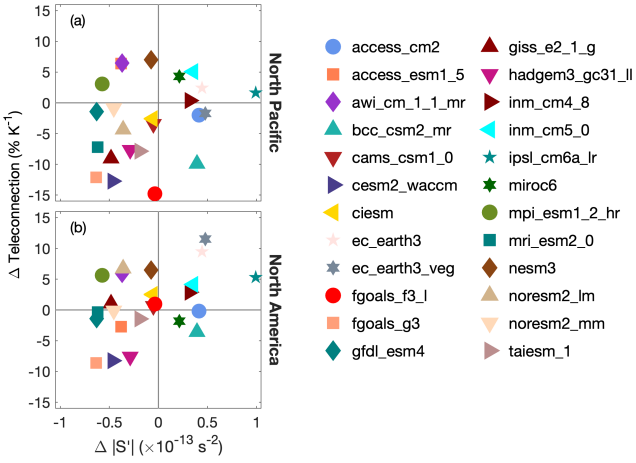

Figure 4. For individual CMIP6 model mean states, the difference in the Rossby wave source (S') versus the difference in the teleconnection amplitude between simulations with historical and future mean state winds for (a) the North Pacific and (b) North America. The horizontal axis is the ensemble-mean, time-mean difference of the absolute value of S' averaged over the subtropical jet (80°-190° E, 20°-40° N).

that uncertainty in the response of the mean state winds to warming dominates uncertainty in modeled changes to the MJO teleconnection.

It is thus important to better understand the cause of teleconnection changes associated with mean state wind changes in the CMIP6 models. Mean state winds can increase or decrease the strength of MJO teleconnections via an intensification of Rossby wave excitation and/or through mean state changes that permit more Rossby wave energy propagation into these regions. The following analysis will argue that the latter–wind-induced changes to Rossby wave ducting–are more important than changes to wave excitation in producing the inter-model teleconnection spread.

To show this, we begin by quantifying the strength of Rossby wave excitation using the linearized equation for the "Rossby wave source" (Sardeshmukh and Hoskins, 1988), S', a term that represents the generation of large-scale vorticity,

$$S' = -\left[\nabla \cdot (\overline{\mathbf{v}_\chi}\zeta') + \nabla \cdot (\mathbf{v}_\chi'\overline{\zeta})\right] \tag{2}$$

where ζ is the absolute vorticity, $\mathbf{v}_\chi$ is the horizontal divergent wind, the overbar represents mean state quantities, and the prime represents anomalies. In the subsequent analysis, we use quantities at 200 hPa to calculate S'.

We do not find a systematic relationship between the difference in S' and the difference in the mean teleconnection amplitude over the North Pacific or North America between simulations with historical and future winds. Figure 4 shows, for simulations with historical and future winds, the relationship between the ensemble mean, time mean, difference in the absolute value of the Rossby wave source averaged over the subtropical jet (80°-190° E, 20°-40° N), and the difference in the mean teleconnection amplitude over the North Pacific and North America. Figure A2 verifies that this region indeed encloses the region of highest S' variability in the LBM simulations. Models with larger increases in $|S'|$ over the jet do not systematically have stronger

https://doi.org/10.5194/wcd-2021-9
Preprint. Discussion started: 10 February 2021

Weather and Climate Dynamics Discussions
Open Access
EGU

teleconnections. If changes to Rossby wave excitation were to play a key role in the difference in the teleconnection amplitude between simulations with historical and future mean state winds, then it would be reasonable to expect either a weaker or similar-sized link over North America than over the North Pacific, since most Rossby waves excited by the MJO propagate first over the Pacific before reaching North America. However, the relationship between the difference in $|S'|$ and the teleconnection amplitude difference appears stronger over North America (r = 0.43) than over the North Pacific (r = 0.27). Thus we conclude that the change in $|S'|$ is not a primary mechanism that explains how mean state winds affect the teleconnection amplitude difference in our LBM simulations.

In addition to playing a key role in Rossby wave excitation, mean state winds also determine the path that Rossby waves take as they propagate (e.g., Karoly, 1983; Hoskins and Ambrizzi, 1993). Analyses of the stationary Rossby wave number have been useful for assessing how the mean state winds affect Rossby wave propagation (e.g., Henderson et al., 2017; Karoly, 1983; Tseng et al., 2020b; Wang et al., 2020). The stationary Rossby wave number on a Mercator projection (to account for spherical geometry) is defined as

$$K_s = a\left(\frac{\beta_M}{u_M}\right)^{1/2}, \tag{3}$$

where β_M is the meridional gradient of absolute vorticity on a Mercator projection,

$$\beta_M = \frac{2\Omega\cos^2\theta}{a} - \frac{\partial}{\partial y}\left[\frac{1}{\cos^2\theta}\frac{\partial}{\partial y}(u_M\cos^2\theta)\right], \tag{4}$$

and $u_M = u/\cos\theta$ is the mean zonal wind divided by the cosine of latitude (θ). In Eqs. (3) and (4), a is the earth's radius and Ω is the earth's rotation rate. Hoskins and Ambrizzi (1993) showed that K_s can be used to understand Rossby wave propagation: waves turn towards regions of higher K_s, are generally reflected away from regions where the zonal Rossby wavelength is equal to K_s or where $\beta_M \leq 0$, and are either dissipated beyond or reflected from regions where $u \leq 0$. Regions of K_s maxima, which tend to occur in strong westerly jets, act as Rossby waveguides. Figure 5a shows K_s computed from the multi-model mean January wind averaged across the historical period. Regions with $\beta_M \leq 0$ are colored black, and regions with $u \leq 0$ are colored white.

Figure 5b,c show the correlation between the changes in the local K_s and the regional mean teleconnection amplitude for the North Pacific and North America, respectively. In the calculation of the correlation, we use averages of the local K_s change over $15^\circ \times 15^\circ$ boxes to focus on the larger features; although using boxes of different sizes does not qualitatively change the results. Regions of strong positive correlation suggest a systematic (common across models) positive relationship between the local change in K_s and the regional (i.e., across North Pacific or North America) teleconnection amplitude change. Similarly, regions of strong negative correlation suggest a systematic inverse relationship between the local change in K_s and the regional teleconnection change. We include boxes outlining the North Pacific and North America regions for reference. Correlations linking regional changes in the local K_s with the regional mean teleconnection amplitude change are generally weaker for the North Pacific than for North America. We thus focus on North America, but point out that the two maps have similar patterns,

https://doi.org/10.5194/wcd-2021-9
Preprint. Discussion started: 10 February 2021

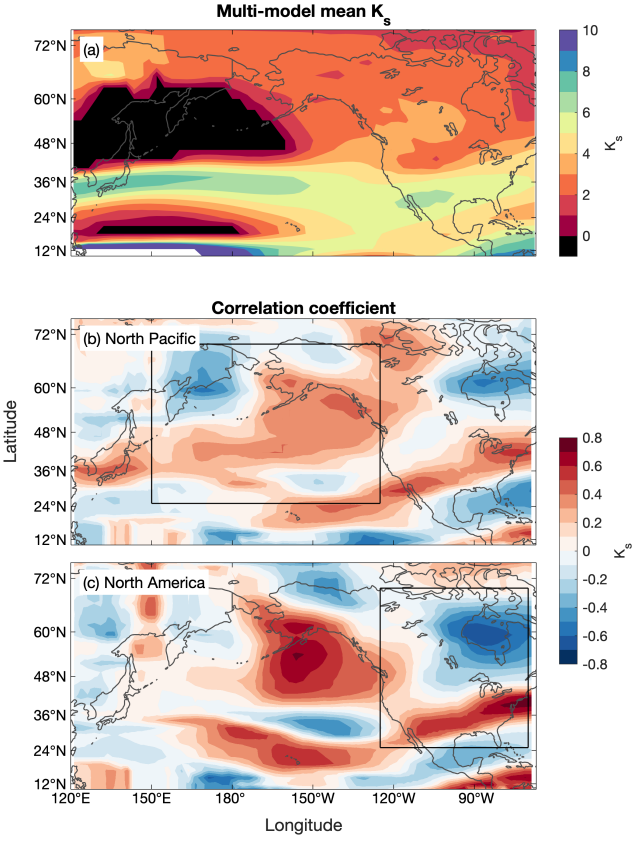

Figure 5. (a) Stationary Rossby wave number, K_s, computed from the multi-model mean wind over the historical period. (b) The correlation coefficient between the local difference in K_s between the historical and future periods, averaged over a $15^\circ \times 15^\circ$ box, and the average teleconnection amplitude change across the North Pacific and (c) North America. Black boxes in (b), (c) outline the North Pacific and North American regions, respectively.

suggesting that changes to the winds leading to stronger teleconnections over North America may be in part due to changes in the winds that also support stronger teleconnections over the North Pacific. Figure 5c shows a region of high positive correlation over the Gulf of Alaska. Here, models exhibiting an increase in K_s tend to have an increase in the teleconnection over North America, and vice versa. Additionally, there is a region of negative correlation just to the south of this area. We interpret this as a slight northward shift and broadening along the northward flank of the Pacific waveguide, and subsequent increase in the number of Rossby waves traveling northward towards North America, in the models that have stronger MJO teleconnections. This view is consistent with the work of Tseng et al. (2020b), who demonstrate how increased K_s over the Gulf of Alaska and resultant increases in northward Rossby wave propagation out of the Pacific waveguide during La Niña years leads to an enhanced MJO teleconnection over North America.

We thus identify a systematic mechanism that may explain how mean state wind changes lead to changes to teleconnectivity over North America across CMIP6 models. This suggests that increased confidence in how winds over this region will change

https://doi.org/10.5194/wcd-2021-9
Preprint. Discussion started: 10 February 2021

in a future climate may help reduce uncertainty in future estimates of the change in the strength of MJO teleconnections to North America. We would like to point out, however, that changes in the winds over this region alone are likely not the sole important change. That is, for some models, it is possible that changes to S' may be important, as well.

3.2 MJO intensity and propagation characteristics

We now investigate how changes to MJO intensity and propagation characteristics affect the MJO teleconnection by conducting simulations in which the mean state is held constant, and either the propagation speed, eastward propagation extent, or intensity of the idealized thermal forcing are perturbed to upper and lower bounds of expected end-of-century changes to the MJO. Instead of using mean states from all CMIP6 models, we use a subset of mean states from 10 models to minimize utilization of computational resources. For these experiments, we chose CMIP6 models that produced a minimum number of unstable ensemble members in experiments used in Sect. 3.1 (see Fig. A1).

Figure 6 summarizes the results of these simulations. Panels a and d show the change to the teleconnection amplitude over the North Pacific and North America, respectively, that result from perturbations to the magnitude of the propagating thermal forcing. The linearity of the LBM ensures that, in the absence of instability, the magnitude of the simulated response varies linearly with the magnitude of the forcing. We verified this with simulations using a 20% increase in the magnitude of the forcing for two different model basic states. For the remainder of the 8 models used in these experiments, we thus did not actually run simulations (see Table 1), because the magnitude of the extratropical response to the perturbed forcing amplitude is independent of the mean state. If full non-linearity had been considered, the variations across the models' mean state could have also been important in the response of the teleconnection.

Unlike perturbations to the heating intensity, the responses of the MJO teleconnection to perturbations to the eastward propagation speed (Fig. 6b,e) and extent (Fig. 6c,f) are linearly sensitive to the mean state. In general, increases to the propagation speed produce modest decreases in the teleconnection strength over the North Pacific, with changes over North America centered on and straddling zero change. Increasing the eastward extent of the propagating MJO thermal forcing in the LBM simulations increases the teleconnection amplitude for all mean states used and has the potential to produce the largest increases in the MJO teleconnection amplitude, more so over the North America region.

Figure 6 highlights two sources of uncertainty that lead to uncertainty in the response of MJO teleconnections to changes to the MJO itself: uncertainty in changes to the MJO and uncertainty in the mean state. Uncertainty in the MJO's response to warming (here, between a 10% overall decrease or 20% overall increase between the present day and end of the 21st century), leads to a range of about 8% K^{-1} uncertainty in the change to the MJO teleconnection to the North Pacific and North America. For the propagation characteristics, both uncertainty in the mean state and uncertainty in the MJO's response to warming leads to uncertainty in the teleconnection response to warming, with a range of about 5% K^{-1} from changes to the MJO's propagation speed and up to about 10% K^{-1} from the MJO's eastward propagation extent. Additionally, for each individual MJO propagation or intensity characteristic, the uncertainty in the MJO teleconnection resulting from a perturbed MJO is on the order of the model uncertainty that results from perturbations to the mean state alone (Fig. 3). This further challenges the notion that it may currently be possible to have confidence in future projections of MJO teleconnections.

https://doi.org/10.5194/wcd-2021-9
Preprint. Discussion started: 10 February 2021

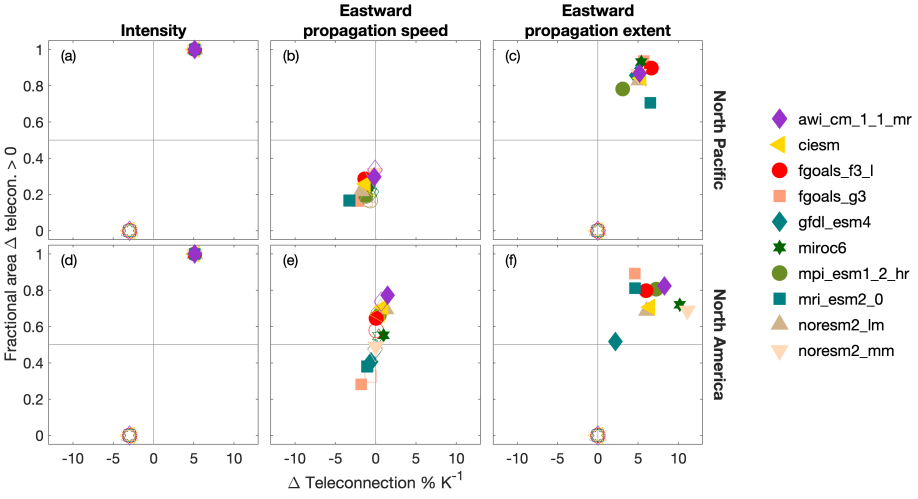

Figure 6. For individual CMIP6 model mean states, the change in the teleconnection amplitude (as a percent change per multi-model mean Kelvin warming) to the North Pacific (150°-235° E, 25°-70° N) and North America (235°-290° E, 25°-70° N) between LBM simulations with the control and perturbed thermal forcing. (a),(d) Response to perturbed heating intensity; (b),(e), eastward propagation speed; and (c),(f), eastward propagation extent. Unfilled (filled) markers represent the lower (upper) bounds of perturbations to each MJO feature expected at the end of the century given a high emissions scenario (see Table 1).

3.3 Sum of mean state and MJO

Putting it together, we finish by quantifying an overall decrease in the MJO teleconnection that results when considering the linear sum of individual changes to the mean state and MJO features. For each CMIP6 model, Fig. 7 shows how the change to the full mean state influences the change in the MJO teleconnection to the North Pacific and North America, as well as the the range of teleconnection changes that results from the sum of changes to the mean state and MJO propagation and intensity characteristics for the 10 CMIP6 mean states for which we also ran perturbed thermal forcing simulations. Over the North Pacific, for all CMIP6 models, changes to the mean state alone lead to an overwhelmingly weaker teleconnection, with only one model (AWI-CM-1-1-MR) showing a small strengthening. When considering also how changes to the MJO may factor in, another model joins in the potential for intensifying teleconnection amplitude. Nonetheless, these results suggest that it is likely that over the North Pacific, in a future warmer climate, MJO teleconnections will weaken.

Over North America, the change in the mean state alone also leads to decreases in the teleconnection amplitude for most CMIP6 models, albeit less so than over the North Pacific, with 3 CMIP6 models showing increases to the MJO teleconnection. When changes to the teleconnection due to changes to the MJO are also considered, the final picture is more blurry, and shows slightly increased potential for strengthening in some models. Over North America, it appears as though changes to the MJO are again likely to weaken MJO teleconnections overall, but with some added uncertainty such that one cannot rule out the possibility of stronger linkages; comparison with Fig. 6 suggests that this is from potential increases due to an intensification and increased eastward propagation extent of the forcing.

https://doi.org/10.5194/wcd-2021-9
Preprint. Discussion started: 10 February 2021

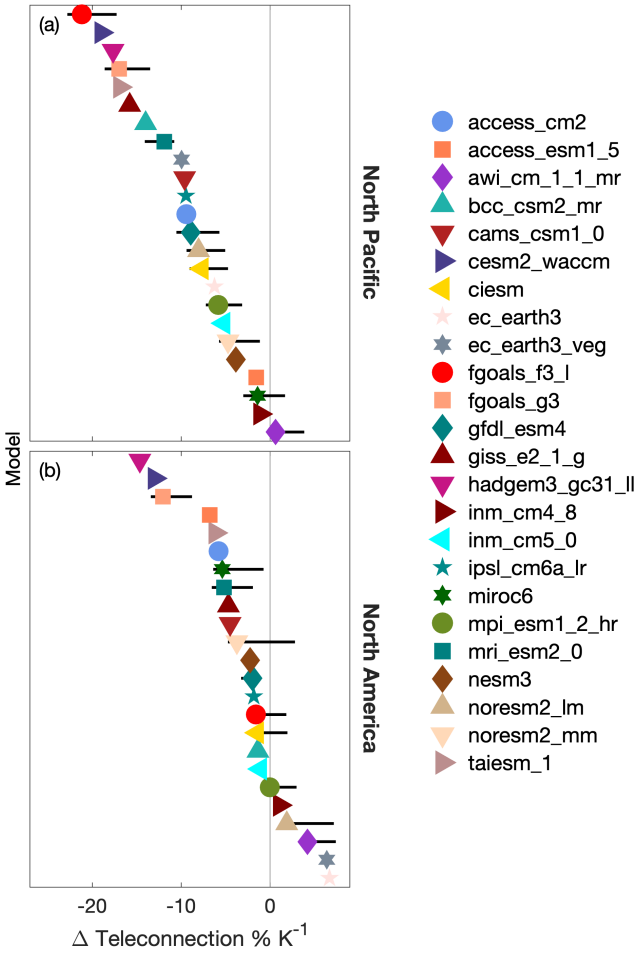

Figure 7. The total change to the MJO teleconnection over (a) the North Pacific and (b) North America due to the change in the full mean state (markers), and the potential range that results from considering changes to MJO propagation and intensity characteristics (horizontal lines extending from each marker) for the 10 models for which we ran perturbed MJO experiments.

4 Conclusions

The Madden-Julian Oscillation (MJO) is a key source of predictability of extratropical weather on subseasonal-to-seasonal timescales. While it is expected that the MJO teleconnection to the extratropics will change in a future warmer climate, models do not agree (Zhou et al., 2020) over much of North America. Speculatively, this may be due in part to mean state biases or due to inter-model spread or biases in the simulation of the MJO, both of which have been shown to lead to biases in the simulated MJO teleconnection of the current climate (Henderson et al., 2017; Wang et al., 2020).

The MJO teleconnection is sensitive to a number of factors, including the large-scale wind and thermal structure of the atmosphere and MJO propagation and intensity characteristics. While a number of climate models simulate the MJO and

https://doi.org/10.5194/wcd-2021-9
Preprint. Discussion started: 10 February 2021

its teleconnections, each model represents a unique combination of multiple changes to the various features of the climate that impact MJO teleconnections. This makes the determination of causal mechanisms important for the change to the MJO teleconnection a challenge. Additionally, many climate models do not accurately reproduce observed characteristics of the MJO or the mean state, and thus may not be reliable for studying internally simulated MJO teleconnections. Previous studies analyzing MJO teleconnections in climate models often analyze a subset of models that produce better MJOs (e.g., Henderson et al., 2017; Zhou et al., 2020).

Motivated by a desire to both (1) untangle the impacts of individual changes to features of the climate on changes to the MJO teleconnection with warming, and (2) maximize the resources offered by the most recent phase of the Coupled Model Intercomparison Project (CMIP6), we conduct a set of sensitivity experiments with a linear baroclinic model (LBM) of the atmosphere in concert with output from CMIP6. In each LBM experiment, a climate feature (i.e., the mean state or intensity or propagation characteristics of a propagating thermal forcing) is perturbed by a climate change amount; that is, the change that is simulated in climate models by the end of the 21st century in simulations with strong CO_2 forcing. Specifically, we test sensitivity of the boreal winter MJO teleconnection strength to the North Pacific and North America to the mean state static stability and winds, and MJO eastward propagation extent, propagation speed, and heating intensity.

As expected, given that the increase of the tropical dry static stability is a robust thermodynamic response to surface warming, we verify that the increase in the tropical dry static stability with warming produces robust decreases in the LBM-simulated MJO teleconnection amplitude. On the other hand, we find relatively large spread in the LBM-simulated teleconnection response to changes in the mean state wind. Nonetheless, when the mean state changes are considered together (Fig. 7), they lead to robust decreases in the MJO teleconnection to the North Pacific. Over North America, the sum of mean state changes leads to a weaker MJO teleconnection for most CMIP6 model mean states, although with many of these models hovering close to zero change.

Investigation into a potential systematic link between changes to the wind and changes to MJO teleconnection revealed a possible connection related to Rossby wave propagation over the eastern Pacific, where models that display increases (decreases) in the stationary wavenumber over the Gulf of Alaska also show increases (decreases) in the teleconnection amplitude over North America.

We find that for perturbations to MJO characteristics (i.e., its intensity, eastward extent, or propagation speed), the uncertainty in the MJO teleconnection that results is on the order of the uncertainty from the mean state changes alone. In particular, increases in the MJO's heating intensity and eastward extent have the potential to lead to large increases in the MJO teleconnection, with the sensitivity to extent being especially strong for teleconnection over North America for some mean states.

Overall, over the North Pacific, despite a relatively large range of -21 to 0.6 % K^{-1}, which depends on the CMIP6 model used as the mean state in the LBM simulations, in general it appears as though the MJO teleconnection to the North Pacific will likely weaken with warming. Over North America, despite a modest multi-model mean weakening result from the influence of the mean state alone, including MJO changes results in many CMIP6 models showing a range of possible teleconnection changes that is either close to or near-zero.

https://doi.org/10.5194/wcd-2021-9
Preprint. Discussion started: 10 February 2021

We have thus identified sources of uncertainty leading to uncertainty in projections of MJO teleconnections in a future warmer climate. To first order, model spread in projections of future winds is the biggest source of uncertainty in projecting the response of MJO teleconnections to warming. For teleconnections to North America in particular, we have identified a region over the eastern Pacific where changes to the winds appear to explain much of the inter-model spread. We speculate that increased confidence in changes to the mean flow over the Gulf of Alaska would help reduce uncertainty in teleconnection changes over North America. Uncertainty in the mean state also affects how MJO teleconnections respond to increases in the eastward extent of MJO convection. Lastly, uncertainty in how the MJO itself will respond to climate change is nontrivial–leading to a range of about 5% K^{-1} for any given mean state (see Fig. 7)–but interestingly secondary to inter-model uncertainty in the wave ducting properties of the basic flow.

Over North America, a possible future outcome is that of the median, near-zero area-mean total teleconnection change. In this case, the pattern of the teleconnection may change, despite zero average change over the region as a whole. In this case, a reduction of the uncertainty in future projections of the mean state winds will still help reduce uncertainty in the MJO teleconnection change, due to the tight dependence of the stationary wave pattern on the mean winds.

We readily admit limitations of our choice of a linear model to explore how the MJO teleconnection responds to changes in the mean state and to the MJO itself. While this allows us to easily diagnose causal relationships, and span a previously sparsely sampled causative parameter space, the linear framework is missing nonlinear relationships between the mean state and the MJO forcing. For example, the mean state exerts a strong control on MJO propagation characteristics (Jiang et al., 2020). The MJO may also play an active role in shaping the midlatitude mean state winds, for example through the modulation of the local Hadley cell (Lyu et al., 2019). Such feedbacks are not simulated in the LBM. Nonetheless, previous work has also shown that the MJO teleconnection is, to first order, linear (Mori and Watanabe, 2008). For now, we suggest this work as a compelling first step towards understanding the intriguing model spread in future MJO teleconnection strength in the extratropics, and another reason to elevate the ongoing community quest to reduce uncertainty of the mean midlatitude circulation's response to climate change.

Code and data availability. Data to reproduce figures is published online at https://zenodo.org/ with doi:10.5281/zenodo.4499184. The linear baroclinic model is available through request from M. Hayashi (michiyah@hawaii.edu). CMIP6 data is publicly available through the Earth System Grid Federation at https://esgf-node.llnl.gov/search/cmip6/.

Appendix A

Figure A1 shows the number of simulations that became unstable (and hence omitted from our analysis; see Sect. 2), and indicates the CMIP6 models for which all simulations were excluded from our analysis for having 10 or more unstable ensemble members for a particular basic state combination.

https://doi.org/10.5194/wcd-2021-9
Preprint. Discussion started: 10 February 2021

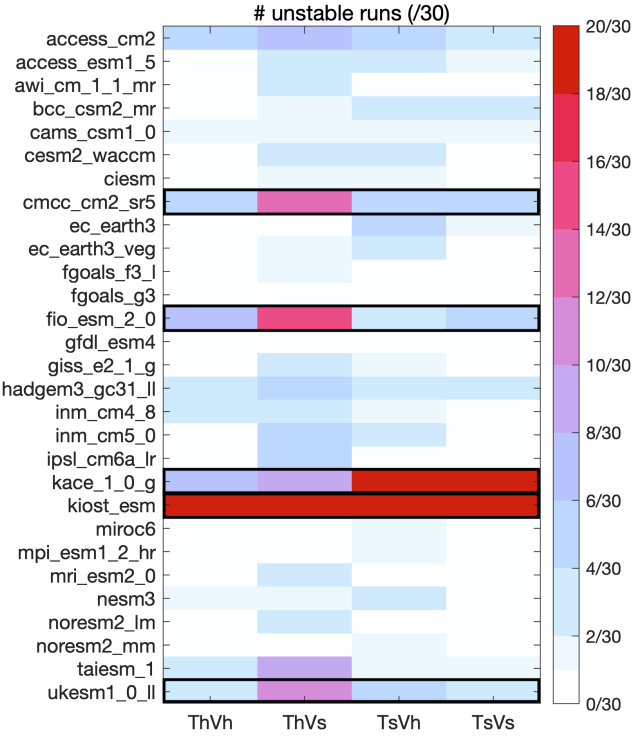

Figure A1. For each model basic state combination, the fraction of the 30 ensemble members that met the instability criterion described in Sect. 2. Models omitted from our analysis (those for which 10 or more of their ensemble members for any of the basic state combinations became unstable) are indicated by the black outline. Th (Ts) = basic state dry static stability from the historical (future) period; Vh (Vs) = basic state winds from the historical (future) period.

Figure A2 shows the temporal variance of the ensemble mean Rossby wave source (S') in the LBM for each CMIP6 model historical basic state used in the analysis. The box around the region (80°-190° E, 20°-40° N) indicates the region used for Fig. 4 of the main text.

https://doi.org/10.5194/wcd-2021-9
Preprint. Discussion started: 10 February 2021

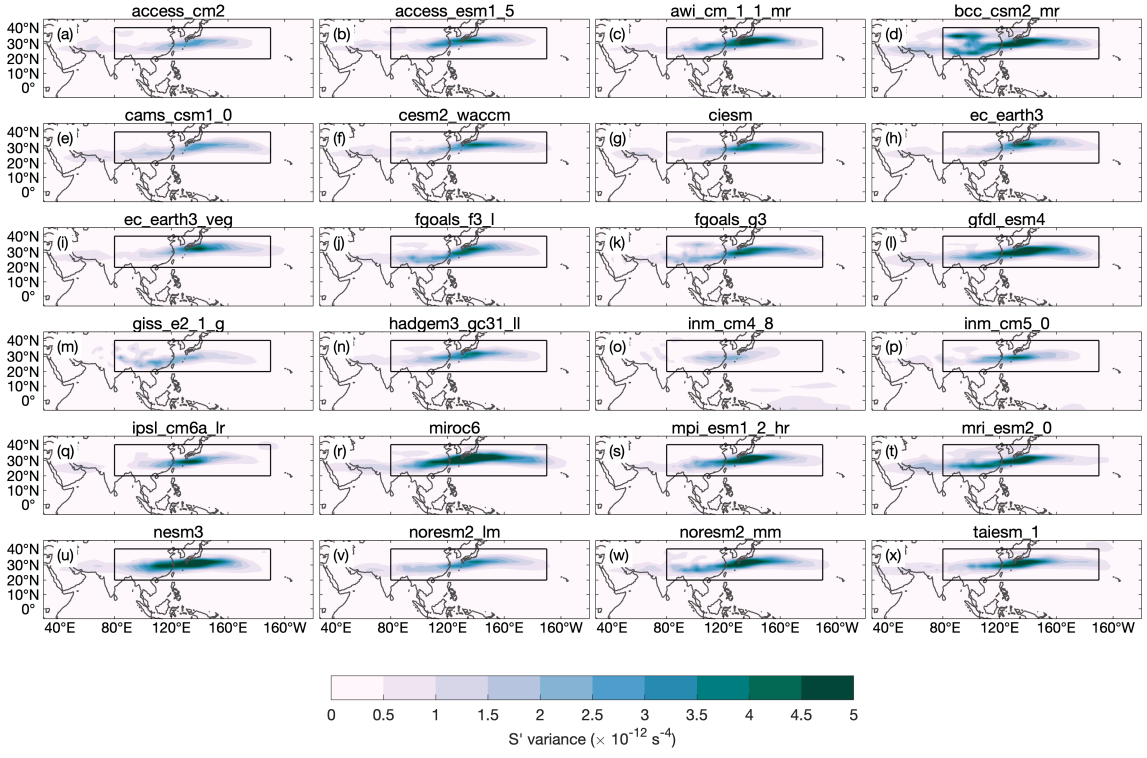

Figure A2. The temporal variance of the ensemble mean Rossby wave source (S') with the full mean states given by historical quantities. The box around the region (80°-190° E, 20°-40° N) indicates the region used for Figure 4 of the main text.

https://doi.org/10.5194/wcd-2021-9
Preprint. Discussion started: 10 February 2021

Weather and Climate Dynamics Discussions
Open Access
EGU

Author contributions. AMJ led the design of the experiments, performed the simulations, and prepared the manuscript. DAR and EAB commented on the manuscript.

Competing interests. The authors declare no competing interests

Acknowledgements. We thank Michiya Hayashi for sending the LBM code, and acknowledge Donald Dazlich, Stephanie Henderson, and Kai-Chih Tseng for their help with setting up the model. We also thank Michael Pritchard for help with manuscript editing and Eric Maloney and Tom Beucler for helpful suggestions. This work was supported by the National Science Foundation under award AGS-1826643, and by the NOAA Climate and Global Change Postdoctoral Fellowship Program, administered by UCAR's Cooperative Programs for the Advancement of Earth System Science (CPAESS) under award NA18NWS4620043B.

This research also used computing resources of the Extreme Science and Engineering Discovery Environment (XSEDE), which is supported by National Science Foundation grand number ACI-1548562 (Towns et al., 2014) and allocation number TG-ATM190002.

https://doi.org/10.5194/wcd-2021-9
Preprint. Discussion started: 10 February 2021

Weather and Climate Dynamics Discussions
Open Access
EGU

References

Adames, Á. F., Kim, D., Sobel, A. H., Del Genio, A., and Wu, J.: Changes in the structure and propagation of the MJO with increasing CO 2 : MJO CHANGES WITH INCREASING CO 2, J. Adv. Model. Earth Syst., 9, 1251–1268, https://doi.org/10.1002/2017MS000913, 2017.

Ahn, M.-S., Kim, D., Sperber, K. R., Kang, I.-S., Maloney, E., Waliser, D., Hendon, H., and on behalf of WGNE MJO Task Force: MJO simulation in CMIP5 climate models: MJO skill metrics and process-oriented diagnosis, Clim. Dyn., 49, 4023–4045, https://doi.org/10.1007/s00382-017-3558-4, 2017.

Bladé, I. and Hartmann, D. L.: The Linear and Nonlinear Extratropical Response of the Atmosphere to Tropical Intraseasonal Heating, J. Atmos. Sci., 52, 4448–4471, https://doi.org/10.1175/1520-0469(1995)052<4448:TLANER>2.0.CO;2, 1995.

Bui, H. X. and Maloney, E. D.: Changes in Madden-Julian Oscillation Precipitation and Wind Variance Under Global Warming, Geophys. Res. Lett., 2018.

Bui, H. X. and Maloney, E. D.: Mechanisms for Global Warming Impacts on Madden–Julian Oscillation Precipitation Amplitude, J. Clim., 32, 6961–6975, https://doi.org/10.1175/JCLI-D-19-0051.1, 2019a.

Bui, H. X. and Maloney, E. D.: Transient Response of MJO Precipitation and Circulation to Greenhouse Gas Forcing, Geophys. Res. Lett., 7, 847, https://doi.org/10.1029/2019GL085328, 2019b.

Chang, C.-W. J., Tseng, W.-L., Hsu, H.-H., Keenlyside, N., and Tsuang, B.-J.: The Madden-Julian Oscillation in a warmer world, Geophys. Res. Lett., 42, 6034–6042, 2015.

Henderson, S. A., Maloney, E. D., and Son, S. W.: Madden-Julian oscillation Pacific teleconnections: The impact of the basic state and MJO representation in general circulation models, J. Clim., 30, 4567–4587, https://doi.org/10.1175/JCLI-D-16-0789.1, 2017.

Hoskins, B. J. and Ambrizzi, T.: Rossby Wave Propagation on a Realistic Longitudinally Varying Flow, J. Atmos. Sci., 50, 1661–1671, https://doi.org/10.1175/1520-0469(1993)050<1661:RWPOAR>2.0.CO;2, 1993.

Jenney, A. M., Randall, D. A., and Barnes, E. A.: Quantifying Regional Sensitivities to Periodic Events: Application to the MJO, J. Geophys. Res. D: Atmos., 44, 7528, https://doi.org/10.1029/2018JD029457, 2019.

Jiang, X., Maloney, E., and Su, H.: Large-scale controls of propagation of the Madden-Julian Oscillation, npj Climate and Atmospheric Science, 3, 1–8, https://doi.org/10.1038/s41612-020-00134-x, 2020.

Karoly, D. J.: Rossby wave propagation in a barotropic atmosphere, Dyn. Atmos. Oceans, 7, 111–125, https://doi.org/10.1016/0377-0265(83)90013-1, 1983.

Lehner, F., Deser, C., Maher, N., Marotzke, J., Fischer, E. M., Brunner, L., Knutti, R., and Hawkins, E.: Partitioning climate projection uncertainty with multiple large ensembles and CMIP5/6, Earth system change: climate scenarios, 11, 491–508, 2020.

Lyu, M., Wu, Z., Shi, X., and Wen, M.: Distinct impacts of the MJO and the NAO on cold wave amplitude in China, Q.J.R. Meteorol. Soc., 145, 1617–1635, https://doi.org/10.1002/qj.3516, 2019.

Maloney, E. D. and Xie, S.-P.: Sensitivity of tropical intraseasonal variability to the pattern of climate warming: MJO ACTIVITY AND CLIMATE WARMING, J. Adv. Model. Earth Syst., 5, 32–47, https://doi.org/10.1029/2012MS000171, 2013.

Maloney, E. D., Adames, Á. F., and Bui, H. X.: Madden–Julian oscillation changes under anthropogenic warming, Nat. Clim. Chang., 9, 26–33, https://doi.org/10.1038/s41558-018-0331-6, 2019.

Mori, M. and Watanabe, M.: The Growth and Triggering Mechanisms of the PNA: A MJO-PNA Coherence, J. Meteorol. Soc. Japan, 86, 213–236, https://doi.org/10.2151/jmsj.86.213, 2008.

https://doi.org/10.5194/wcd-2021-9
Preprint. Discussion started: 10 February 2021

Moss, R. H., Edmonds, J. A., Hibbard, K. A., Manning, M. R., Rose, S. K., van Vuuren, D. P., Carter, T. R., Emori, S., Kainuma, M., Kram, T., Meehl, G. A., Mitchell, J. F. B., Nakicenovic, N., Riahi, K., Smith, S. J., Stouffer, R. J., Thomson, A. M., Weyant, J. P., and Wilbanks, T. J.: The next generation of scenarios for climate change research and assessment, Nature, 463, 747–756, 2010.

O'Neill, B. C., Kriegler, E., Ebi, K. L., Kemp-Benedict, E., Riahi, K., Rothman, D. S., van Ruijven, B. J., van Vuuren, D. P., Birkmann, J., Kok, K., Levy, M., and Solecki, W.: The roads ahead: Narratives for shared socioeconomic pathways describing world futures in the 21st century, Glob. Environ. Change, 42, 169–180, 2017.

Robertson, A. W., Kumar, A., Peña, M., and Vitart, F.: Improving and promoting subseasonal to seasonal prediction, Bull. Am. Meteorol. Soc., 96, ES49–ES53, https://doi.org/10.1175/BAMS-D-14-00139.1, 2015.

Rushley, S. S., Kim, D., and Adames, Á. F.: Changes in the MJO under Greenhouse Gas–Induced Warming in CMIP5 Models, J. Clim., 32, 803–821, https://doi.org/10.1175/JCLI-D-18-0437.1, 2019.

Sardeshmukh, P. D. and Hoskins, B. J.: The Generation of Global Rotational Flow by Steady Idealized Tropical Divergence, https://doi.org/10.1175/1520-0469(1988)045<1228:TGOGRF>2.0.CO;2, 1988.

Seo, K.-H. and Lee, H.-J.: Mechanisms for a PNA-Like Teleconnection Pattern in Response to the MJO, J. Atmos. Sci., 74, 1767–1781, https://doi.org/10.1175/JAS-D-16-0343.1, 2017.

Seo, K.-H. and Son, S.-W.: The Global Atmospheric Circulation Response to Tropical Diabatic Heating Associated with the Madden–Julian Oscillation during Northern Winter, J. Atmos. Sci., 69, 79–96, https://doi.org/10.1175/2011JAS3686.1, 2012.

Seo, K.-H., Lee, H.-J., and Frierson, D. M. W.: Unraveling the Teleconnection Mechanisms that Induce Wintertime Temperature Anomalies over the Northern Hemisphere Continents in Response to the MJO, J. Atmos. Sci., 73, 3557–3571, https://doi.org/10.1175/JAS-D-16-0036.1, 2016.

Subramanian, A., Jochum, M., Miller, A. J., Neale, R., Seo, H., Waliser, D., and Murtugudde, R.: The MJO and global warming: A study in CCSM4, Clim. Dyn., 42, 2019–2031, https://doi.org/10.1007/s00382-013-1846-1, 2014.

Towns, J., Cockerill, T., Dahan, M., Foster, I., Gaither, K., Grimshaw, A., Hazlewood, V., Lathrop, S., Lifka, D., Peterson, G. D., Roskies, R., Scott, J. R., and Wilkins-Diehr, N.: XSEDE: Accelerating Scientific Discovery, Computing in Science Engineering, 16, 62–74, 2014.

Tseng, K.-C., Maloney, E., and Barnes, E.: The Consistency of MJO Teleconnection Patterns: An Explanation Using Linear Rossby Wave Theory, J. Clim., 32, 531–548, https://doi.org/10.1175/JCLI-D-18-0211.1, 2019.

Tseng, K.-C., Barnes, E. A., and Maloney, E.: The Importance of Past MJO Activity in Determining the Future State of the Midlatitude Circulation, J. Clim., 33, 2131–2147, 2020a.

Tseng, K.-C., Maloney, E., and Barnes, E. A.: The Consistency of MJO Teleconnection Patterns on Interannual Time Scales, J. Clim., 33, 3471–3486, https://doi.org/10.1175/JCLI-D-19-0510.1, 2020b.

Wang, J., Kim, H., Kim, D., Henderson, S. A., Stan, C., and Maloney, E. D.: MJO Teleconnections over the PNA Region in Climate Models. Part II: Impacts of the MJO and Basic State, J. Clim., 33, 5081–5101, 2020.

Watanabe, M. and Kimoto, M.: Atmosphere-ocean thermal coupling in the North Atlantic: A positive feedback, Q.J Royal Met. Soc., 126, 3343–3369, https://doi.org/10.1002/qj.49712657017, 2000.

Wolding, B. O., Maloney, E. D., and Branson, M.: Vertically resolved weak temperature gradient analysis of the Madden-Julian Oscillation in SP-CESM: WTG ANALYSIS OF THE MJO IN SP-CESM, J. Adv. Model. Earth Syst., 8, 1586–1619, https://doi.org/10.1002/2016MS000724, 2016.

https://doi.org/10.5194/wcd-2021-9
Preprint. Discussion started: 10 February 2021

Wolding, B. O., Maloney, E. D., Henderson, S., and Branson, M.: Climate change and the Madden-Julian Oscillation: A vertically resolved weak temperature gradient analysis: CLIMATE CHANGE AND THE MJO, Journal of Advances in Modeling Earth Systems, 9, 307–331, https://doi.org/10.1002/2016MS000843, 2017.

Zhou, S., L'Heureux, M., Weaver, S., and Kumar, A.: A composite study of the MJO influence on the surface air temperature and precipitation over the Continental United States, Clim. Dyn., 38, 1459–1471, 2012.

Zhou, W., Yang, D., Xie, S.-P., and Ma, J.: Amplified Madden–Julian oscillation impacts in the Pacific–North America region, Nat. Clim. Chang., https://doi.org/10.1038/s41558-020-0814-0, 2020.